Structural Analysis Equations

Douglas R. Rammer, Research General Engineer

Contents

Equations for deformation and stress, which are the basis for tension members and beam and column design, are discussed in this chapter. The first two sections cover tapered members, straight members, and special considerations such as notches, slits, and size effect. A third section presents stability criteria for members subject to buckling and for members subject to special conditions.

Note that this chapter focuses primarily on presenting fundamental mechanics-based equations. For design procedures, the reader is encouraged to contact appropriate industry trade associations or product manufacturers. Current design information can be readily obtained form their web sites, technical handbooks, and bulletins.

Deformation Equations

Equations for deformation of wood members are presented as functions of applied loads, moduli of elasticity and rigidity, and member dimensions. They may be solved to determine minimum required cross-sectional dimensions to meet deformation limitations imposed in design. Average moduli of elasticity and rigidity are given in Chapter 5. Consideration must be given to variability in material properties and uncertainties in applied loads to control reliability of the design.

Axial Load

The deformation of an axially loaded member is not usually an important design consideration. More important considerations will be presented in later sections dealing with combined loads or stability. Axial load produces a change of length given by

$$\delta = \frac{PL}{AE} \tag{9–1}$$

where δ is change of length, L length, A cross-sectional area, E modulus of elasticity (E_L when grain runs parallel to member axis), and P axial force parallel to grain.

Bending

Straight Beam Deflection

The deflection of straight beams that are elastically stressed and have a constant cross section throughout their length is given by

$$\delta = \frac{k_b W L^3}{EI} + \frac{k_s W L}{GA'} \tag{9–2}$$

where δ is deflection, W total beam load acting perpendicular to beam neutral axis, L beam span, k_b and k_s constants

Table 9–1. Values of k_b and k_s for several beam loadings

Loading	Beam ends	Deflection at	k_b	k_s
Uniformly distributed	Both simply supported	Midspan	5/384	1/8
	Both clamped	Midspan	1/384	1/8
Concentrated at midspan	Both simply supported	Midspan	1/48	1/4
	Both clamped	Midspan	1/192	1/4
Concentrated at outer quarter span points	Both simply supported	Midspan	11/768	1/8
	Both simply supported	Load point	1/96	1/8
Uniformly distributed	Cantilever, one free, one clamped	Free end	1/8	1/2
Concentrated at free end	Cantilever, one free, one clamped	Free end	1/3	1

dependent upon beam loading, support conditions, and location of point whose deflection is to be calculated, I beam moment of inertia, A' modified beam area, E beam modulus of elasticity (for beams having grain direction parallel to their axis, $E = E_L$), and G beam shear modulus (for beams with flat-grained vertical faces, $G = G_{LT}$, and for beams with edge-grained vertical faces, $G = G_{LR}$). Elastic property values are given in Tables 5–1 and 5–2 (Chap. 5). The first term on the right side of Equation (9–2) gives the bending deflection and the second term the shear deflection. Values of k_b and k_s for several cases of loading and support are given in Table 9–1.

The moment of inertia I of the beams is given by

$$I = \frac{bh^3}{12} \quad \text{for beam of rectangular cross section}$$
$$= \frac{\pi d^4}{64} \quad \text{for beam of circular cross section} \tag{9–3}$$

where b is beam width, h beam depth, and d beam diameter. The modified area A' is given by

$$A' = \frac{5}{6}bh \quad \text{for beam of rectangular cross section}$$
$$= \frac{9}{40}\pi d^2 \quad \text{for beam of circular cross section} \tag{9–4}$$

If the beam has initial deformations such as bow (lateral bend) or twist, these deformations will be increased by the bending loads. It may be necessary to provide lateral or torsional restraints to hold such members in line. (See Interaction of Buckling Modes section.)

Tapered Beam Deflection

Figures 9–1 and 9–2 are useful in the design of tapered beams. The ordinates are based on design criteria such as span, loading, difference in beam height ($h_c - h_0$) as required by roof slope or architectural effect, and maximum allowable deflection, together with material properties. From this, the value of the abscissa can be determined and the smallest beam depth h_0 can be calculated for comparison with that given by the design criteria. Conversely, the deflection of a beam can be calculated if the value of the abscissa is known. Tapered beams deflect as a result of shear deflection in addition to bending deflections (Figs. 9–1 and 9–2), and this

shear deflection Δ_s can be closely approximated by

$$\Delta_s = \frac{3WL}{20Gbh_0} \quad \text{for uniformly distributed load}$$
$$= \frac{3PL}{10Gbh_0} \quad \text{for midspan-concentrated load} \tag{9–5}$$

The final beam design should consider the total deflection as the sum of the shear and bending deflection, and it may be necessary to iterate to arrive at final beam dimensions. Equations (9–5) are applicable to either single-tapered or double-tapered beams. As with straight beams, lateral or torsional restraint may be necessary.

Effect of Notches and Holes

The deflection of beams is increased if reductions in cross-section dimensions occur, such as by holes or notches. The deflection of such beams can be determined by considering them of variable cross section along their length and appropriately solving the general differential equations of the elastic curves, $EI(d^2y/dx^2) = M$, to obtain deflection expressions or by the application of Castigliano's theorem. (These procedures are given in most texts on strength of materials.)

Effect of Time: Creep Deflections

In addition to the elastic deflections previously discussed, wood beams usually sag in time; that is, the deflection increases beyond what it was immediately after the load was first applied. (See the discussion of creep in Time under Load in Chap. 5.)

Green timbers, in particular, will sag if allowed to dry under load, although partially dried material will also sag to some extent. In thoroughly dried beams, small changes in deflection occur with changes in moisture content but with little permanent increase in deflection. If deflection under longtime load with initially green timber is to be limited, it has been customary to design for an initial deflection of about half the value permitted for longtime deflection. If deflection under longtime load with initially dry timber is to be limited, it has been customary to design for an initial deflection of about two-thirds the value permitted for longtime deflection.

Water Ponding

Ponding of water on roofs already deflected by other loads can cause large increases in deflection. The total short-term
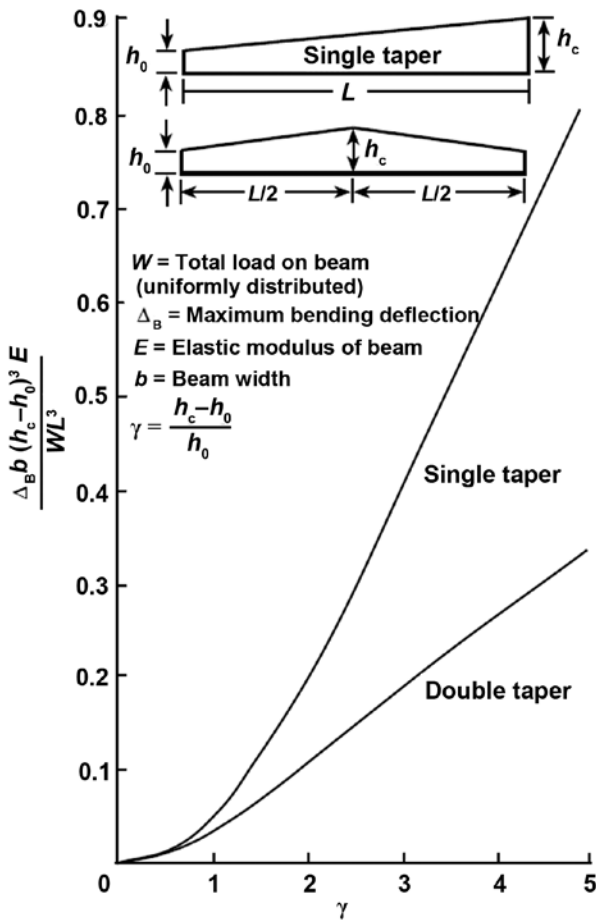
Figure 9–1. Graph for determining tapered beam size based on deflection under uniformly distributed load.

Figure 9–2. Graph for determining tapered beam size on deflection under concentrated midspan load.

deflection Δ due to design load plus ponded water can be closely estimated by

$$\Delta = \frac{\Delta_0}{1 - S/S_{cr}} \qquad (9\text{–}6)$$

where Δ_0 is deflection due to design load alone, S beam spacing, and S_{cr} critical beam spacing (Eq. (9–31)).

Combined Bending and Axial Load

Concentric Load

Addition of a concentric axial load to a beam under loads acting perpendicular to the beam neutral axis causes increase in bending deflection for added axial compression and decrease in bending deflection for added axial tension. The deflection under combined loading at midspan for pin-ended members can be estimated closely by

$$\Delta = \frac{\Delta_0}{1 \pm P/P_{cr}} \qquad (9\text{–}7)$$

where the plus sign is chosen if the axial load is tension and the minus sign if the axial load is compression, Δ is midspan deflection under combined loading, Δ_0 beam midspan deflection without axial load, P axial load, and
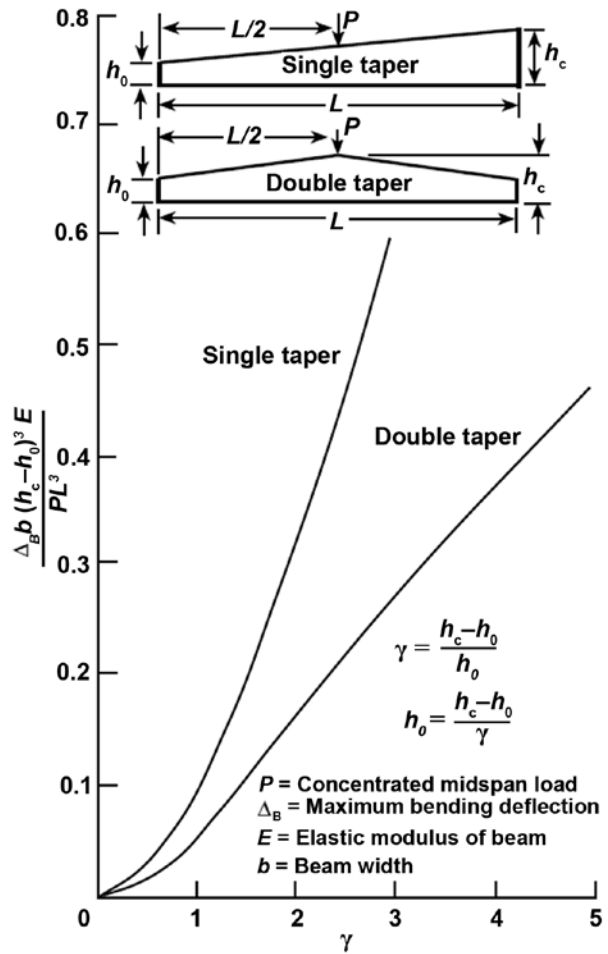
P_{cr} a constant equal to the buckling load of the beam under axial compressive load only (see Axial Compression in Stability Equations section.) based on flexural rigidity about the neutral axis perpendicular to the direction of bending loads. This constant appears regardless of whether P is tension or compression. If P is compression, it must be less than P_{cr} to avoid collapse. When the axial load is tension, it is conservative to ignore the P/P_{cr} term. (If the beam is not supported against lateral deflection, its buckling load should be checked using Eq. (9–35).)

Eccentric Load

If an axial load is eccentrically applied to a pin-ended member, it will induce bending deflections and change in length given by Equation (9–1). Equation (9–7) can be applied to find the bending deflection by writing the equation in the form

$$\delta_b + \varepsilon_0 = \frac{\varepsilon_0}{1 \pm P/P_{cr}} \qquad (9\text{–}8)$$

where δ_b is the induced bending deflection at midspan and ε_0 the eccentricity of P from the centroid of the cross section.
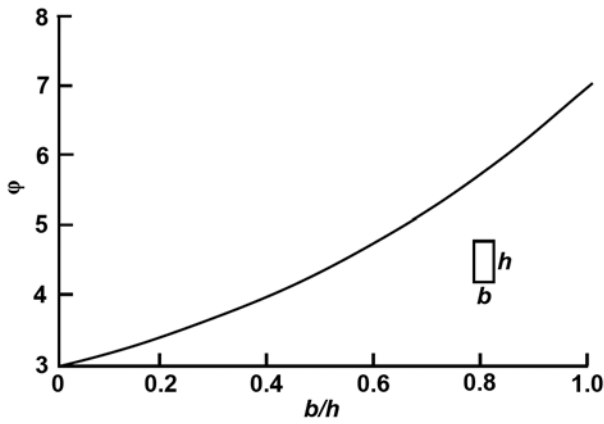
Figure 9–3. Coefficient φ for determining torsional rigidity of rectangular member (Eq. (9 –11)).

Torsion

The angle of twist of wood members about the longitudinal axis can be computed by

$$\theta = \frac{TL}{GK} \tag{9–9}$$

where θ is angle of twist in radians, T applied torque, L member length, G shear modulus (use $\sqrt{G_{LR}G_{LT}}$, or approximate G by $E_L/16$ if measured G is not available), and K a cross-section shape factor. For a circular cross section, K is the polar moment of inertia:

$$K = \frac{\pi D^4}{32} \tag{9–10}$$

where D is diameter. For a rectangular cross section,

$$K = \frac{hb^3}{\varphi} \tag{9–11}$$

where h is larger cross-section dimension, b is smaller cross-section dimension, and φ is given in Figure 9–3.

Stress Equations

The equations presented here are limited by the assumption that stress and strain are directly proportional (Hooke's law) and by the fact that local stresses in the vicinity of points of support or points of load application are correct only to the extent of being statically equivalent to the true stress distribution (St. Venant's principle). Local stress concentrations must be separately accounted for if they are to be limited in design.

Axial Load

Tensile Stress

Concentric axial load (along the line joining the centroids of the cross sections) produces a uniform stress:

$$f_t = \frac{P}{A} \tag{9–12}$$

where f_t is tensile stress, P axial load, and A cross-sectional area.

Short-Block Compressive Stress

Equation (9–12) can also be used in compression if the member is short enough to fail by simple crushing without deflecting laterally. Such fiber crushing produces a local "wrinkle" caused by microstructural instability. The member as a whole remains structurally stable and able to bear load.

Bending

The strength of beams is determined by flexural stresses caused by bending moment, shear stresses caused by shear load, and compression across the grain at the end bearings and load points.

Straight Beam Stresses

The stress due to bending moment for a simply supported pin-ended beam is a maximum at the top and bottom edges. The concave edge is compressed, and the convex edge is under tension. The maximum stress is given by

$$f_b = \frac{M}{Z} \tag{9–13}$$

where f_b is bending stress, M bending moment, and Z beam section modulus (for a rectangular cross section, $Z = bh^2/6$; for a circular cross section, $Z = \pi D^3/32$).

This equation is also used beyond the limits of Hooke's law with M as the ultimate moment at failure. The resulting pseudo-stress is called the "modulus of rupture," values of which are tabulated in Chapter 5. The modulus of rupture has been found to decrease with increasing size of member. (See Size Effect section.)

The shear stress due to bending is a maximum at the centroidal axis of the beam, where the bending stress happens to be zero. (This statement is not true if the beam is tapered—see following section.) In wood beams this shear stress may produce a failure crack near mid-depth running along the axis of the member. Unless the beam is sufficiently short and deep, it will fail in bending before shear failure can develop; but wood beams are relatively weak in shear, and shear strength can sometimes govern a design. The maximum shear stress is

$$f_s = k\frac{V}{A} \tag{9–14}$$

where f_s is shear stress, V vertical shear force on cross section, A cross-sectional area, and $k = 3/2$ for a rectangular cross section or $k = 4/3$ for a circular cross section.

Tapered Beam Stresses

For beams of constant width that taper in depth at a slope less than 25°, the bending stress can be obtained from Equation (9–13) with an error of less than 5%. The shear stress, however, differs markedly from that found in uniform beams. It can be determined from the basic theory presented
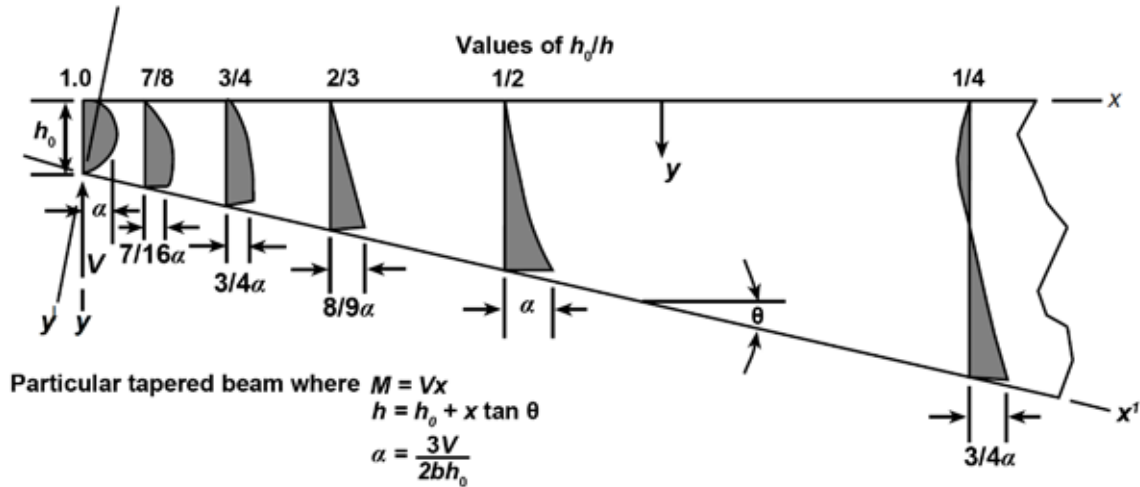
Figure 9–4. Shear stress distribution for a tapered beam.

by Maki and Kuenzi (1965). The shear stress at the tapered edge can reach a maximum value as great as that at the neutral axis at a reaction.

Consider the example shown in Figure 9–4, in which concentrated loads farther to the right have produced a support reaction V at the left end. In this case the maximum stresses occur at the cross section that is double the depth of the beam at the reaction. For other loadings, the location of the cross section with maximum shear stress at the tapered edge will be different.

For the beam depicted in Figure 9–4, the bending stress is also a maximum at the same cross section where the shear stress is maximum at the tapered edge. This stress situation also causes a stress in the direction perpendicular to the neutral axis that is maximum at the tapered edge. The effect of combined stresses at a point can be approximately accounted for by an interaction equation based on the Henky–von Mises theory of energy due to the change of shape. This theory applied by Norris (1950) to wood results in

$$\frac{f_x^2}{F_x^2} + \frac{f_{xy}^2}{F_{xy}^2} + \frac{f_y^2}{F_y^2} = 1 \qquad (9\text{–}15)$$

where f_x is bending stress, f_y stress perpendicular to the neutral axis, and f_{xy} shear stress. Values of F_x, F_y, and F_{xy} are corresponding stresses chosen at design values or maximum values in accordance with allowable or maximum values being determined for the tapered beam. Maximum stresses in the beam depicted in Figure 9–4 are given by

$$f_x = \frac{3M}{2bh_0^2}$$
$$f_{xy} = f_x \tan \theta \qquad (9\text{–}16)$$
$$f_y = f_x \tan^2 \theta$$

Substitution of these equations into the interaction Equation (9–15) will result in an expression for the moment capacity

M of the beam. If the taper is on the beam tension edge, the values of f_x and f_y are tensile stresses.

Example: Determine the moment capacity (newton-meters) of a tapered beam of width $b = 100$ mm, depth $h_0 = 200$ mm, and taper $\tan \theta = 1/10$. Substituting these dimensions into Equation (9–16) (with stresses in pascals) results in

$$f_x = 375M$$
$$f_{xy} = 37.5M$$
$$f_y = 3.75M$$

Substituting these into Equation (9–15) and solving for M results in

$$M = \frac{1}{3.75 \left[10^4 / F_x^2 + 10^2 / F_{xy}^2 + 1 / F_y^2 \right]^{1/2}}$$

where appropriate allowable or maximum values of the F stresses are chosen.

Size Effect

The modulus of rupture (maximum bending stress) of wood beams depends on beam size and method of loading, and the strength of clear, straight-grained beams decreases as size increases. These effects were found to be describable by statistical strength theory involving "weakest link" hypotheses and can be summarized as follows: For two beams under two equal concentrated loads applied symmetrical to the midspan points, the ratio of the modulus of rupture of beam 1 to the modulus of rupture of beam 2 is given by

$$\frac{R_1}{R_2} = \left[\frac{h_2 L_2 (1 + ma_2 / L_2)}{h_1 L_1 (1 + ma_1 / L_1)} \right]^{1/m} \qquad (9\text{–}17)$$

where subscripts 1 and 2 refer to beam 1 and beam 2, R is modulus of rupture, h beam depth, L beam span, a distance between loads placed $a/2$ each side of midspan, and m a constant. For clear, straight-grained Douglas-fir beams, $m = 18$. If Equation (9–17) is used for beam 2 size (Chap. 5)

loaded at midspan, then $h_2 = 5.08$ mm (2 in.), $L_2 = 71.112$ mm (28 in.), and $a_2 = 0$ and Equation (9–17) becomes

$$\frac{R_1}{R_2} = \left[\frac{361.29}{h_1 L_1(1 + ma_1/L_1)}\right]^{1/m} \quad \text{(metric)} \quad (9\text{–}18a)$$

$$\frac{R_1}{R_2} = \left[\frac{56}{h_1 L_1(1 + ma_1/L_1)}\right]^{1/m} \quad \text{(inch–pound)} \quad (9\text{–}18b)$$

Example: Determine modulus of rupture for a beam 10 in. deep, spanning 18 ft, and loaded at one-third span points compared with a beam 2 in. deep, spanning 28 in., and loaded at midspan that had a modulus of rupture of 10,000 lb in^{-2}. Assume $m = 18$. Substituting the dimensions into Equation (9–18) produces

$$R_1 = 10,000\left[\frac{56}{2,160(1+6)}\right]^{1/18}$$

$$= 7,330 \text{ lb in}^{-2}$$

Application of the statistical strength theory to beams under uniformly distributed load resulted in the following relationship between modulus of rupture of beams under uniformly distributed load and modulus of rupture of beams under concentrated loads:

$$\frac{R_u}{R_c} = \left[\frac{(1 + 18a_c/L_c)h_c L_c}{3.876 h_u L_u}\right]^{1/18} \quad (9\text{–}19)$$

where subscripts u and c refer to beams under uniformly distributed and concentrated loads, respectively, and other terms are as previously defined.

Shear strength for non-split, non-checked, solid-sawn, and glulam beams also decreases as beam size increases. A relationship between beam shear τ and ASTM shear block strength τ_{ASTM}, including a stress concentration factor for the re-entrant corner of the shear block, C_f, and the shear area A, is

$$\tau = \frac{1.9 C_f \tau_{ASTM}}{A^{1/5}} \quad \text{(metric)} \quad (9\text{–}20a)$$

$$\tau = \frac{1.3 C_f \tau_{ASTM}}{A^{1/5}} \quad \text{(inch–pound)} \quad (9\text{–}20b)$$

where τ is beam shear (MPa, lb in^{-2}), C_f stress concentration factor, τ_{ASTM} ASTM shear block strength (MPa, lb in^{-2}), and A shear area (cm^2, in^2).

This relationship was determined by empirical fit to test data. The shear block re-entrant corner concentration factor is approximately 2; the shear area is defined as beam width multiplied by the length of beam subjected to shear force.

Effect of Notches, Slits, and Holes

In beams having notches, slits, or holes with sharp interior corners, large stress concentrations exist at the corners. The local stresses include shear parallel to grain and tension perpendicular to grain. As a result, even moderately low loads can cause a crack to initiate at the sharp corner and propagate along the grain. An estimate of the crack-initiation load
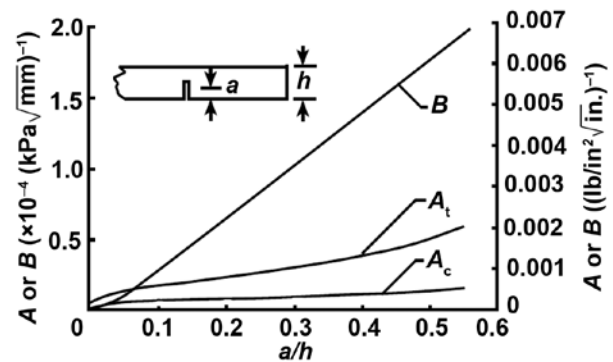

Figure 9–5. Coefficients *A* and *B* for crack-initiation criterion (Eq. (9–21)).

can be obtained by the fracture mechanics analysis of Murphy (1979) for a beam with a slit, but it is generally more economical to avoid sharp notches entirely in wood beams, especially large wood beams, since there is a size effect: sharp notches cause greater reductions in strength for larger beams. A conservative criterion for crack initiation for a beam with a slit is

$$\sqrt{h}\left[A\left(\frac{6M}{bh^2}\right) + B\left(\frac{3V}{2bh}\right)\right] = 1 \quad (9\text{–}21)$$

where h is beam depth, b beam width, M bending moment, and V vertical shear force, and coefficients A and B are presented in Figure 9–5 as functions of a/h, where a is slit depth. The value of A depends on whether the slit is on the tension edge or the compression edge. Therefore, use either A_t or A_c as appropriate. The values of A and B are dependent upon species; however, the values given in Figure 9–5 are conservative for most softwood species.

Effects of Time: Creep Rupture, Fatigue, and Aging

See Chapter 5 for a discussion of fatigue and aging. Creep rupture is accounted for by duration-of-load adjustment in the setting of allowable stresses, as discussed in Chapters 5 and 7.

Water Ponding

Ponding of water on roofs can cause increases in bending stresses that can be computed by the same amplification factor (Eq. (9–6)) used with deflection. (See Water Ponding in the Deformation Equations section.)

Combined Bending and Axial Load

Concentric Load

Equation (9–7) gives the effect on deflection of adding an end load to a simply supported pin-ended beam already bent by transverse loads. The bending stress in the member is modified by the same factor as the deflection:

$$f_b = \frac{f_{b0}}{1 \pm P/P_{cr}} \quad (9\text{–}22)$$

where the plus sign is chosen if the axial load is tension and the minus sign is chosen if the axial load is compression, f_b is net bending stress from combined bending and axial load, f_{b0} bending stress without axial load, P axial load, and P_{cr} the buckling load of the beam under axial compressive load only (see Axial Compression in the Stability Equations section), based on flexural rigidity about the neutral axis perpendicular to the direction of the bending loads. This P_{cr} is not necessarily the minimum buckling load of the member. If P is compressive, the possibility of buckling under combined loading must be checked. (See Interaction of Buckling Modes.)

The total stress under combined bending and axial load is obtained by superposition of the stresses given by Equations (9–12) and (9–22).

Example: Suppose transverse loads produce a bending stress f_{b0} tensile on the convex edge and compressive on the concave edge of the beam. Then the addition of a tensile axial force P at the centroids of the end sections will produce a maximum tensile stress on the convex edge of

$$f_{t\,max} = \frac{f_{b0}}{1 + P/P_{cr}} + \frac{P}{A}$$

and a maximum compressive stress on the concave edge of

$$f_{c\,max} = \frac{f_{b0}}{1 + P/P_{cr}} - \frac{P}{A}$$

where a negative result would indicate that the stress was in fact tensile.

Eccentric Load

If the axial load is eccentrically applied, then the bending stress f_{b0} should be augmented by $\pm P\varepsilon_0/Z$, where ε_0 is eccentricity of the axial load.

Example: In the preceding example, let the axial load be eccentric toward the concave edge of the beam. Then the maximum stresses become

$$f_{t\,max} = \frac{f_{b0} - P\varepsilon_0/Z}{1 + P/P_{cr}} + \frac{P}{A}$$

$$f_{c\,max} = \frac{f_{b0} - P\varepsilon_0/Z}{1 + P/P_{cr}} - \frac{P}{A}$$

Torsion

For a circular cross section, the shear stress induced by torsion is

$$f_s = \frac{16T}{\pi D^3} \qquad (9\text{–}23)$$

where T is applied torque and D diameter. For a rectangular cross section,

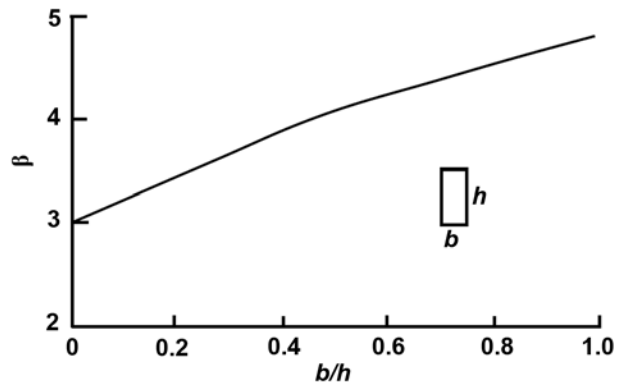$$f_s = \frac{T}{\beta h b^2} \qquad (9\text{–}24)$$

Figure 9–6. Coefficient β for computing maximum shear stress in torsion of rectangular member (Eq. (9–24)).

where T is applied torque, h larger cross-section dimension, and b smaller cross-section dimension, and β is presented in Figure 9–6.

Stability Equations

Axial Compression

For slender members under axial compression, stability is the principal design criterion. The following equations are for concentrically loaded members. For eccentrically loaded columns, see Interaction of Buckling Modes section.

Long Columns

A column long enough to buckle before the compressive stress P/A exceeds the proportional limit stress is called a "long column." The critical stress at buckling is calculated by Euler's formula:

$$f_{cr} = \frac{\pi^2 E_L}{(L/r)^2} \qquad (9\text{–}25)$$

where E_L is elastic modulus parallel to the axis of the member, L unbraced length, and r least radius of gyration (for a rectangular cross section with b as its least dimension, $r = b/\sqrt{12}$, and for a circular cross section, $r = d/4$). Equation (9–25) is based on a pinned-end condition but may be used conservatively for square ends as well.

Short Columns

Columns that buckle at a compressive stress P/A beyond the proportional limit stress are called "short columns." Usually the short column range is explored empirically, and appropriate design equations are proposed. Material of this nature is presented in *USDA Technical Bulletin 167* (Newlin and Gahagan 1930). The final equation is a fourth-power parabolic function that can be written as

$$f_{cr} = F_c \left[1 - \frac{4}{27\pi^4} \left(\frac{L}{r} \sqrt{\frac{F_c}{E_L}} \right)^4 \right] \qquad (9\text{–}26)$$

where F_c is compressive strength and remaining terms are defined as in Equation (9–25). Figure 9–7 is a graphical representation of Equations (9–25) and (9–26).

Short columns can be analyzed by fitting a nonlinear function to compressive stress–strain data and using it in place of Hooke's law. One such nonlinear function proposed by Ylinen (1956) is

$$\varepsilon = \frac{F_c}{E_L}\left[c\frac{f}{F_c} - (1-c)\log_e\left(1 - \frac{f}{F_c}\right)\right] \qquad (9\text{–}27)$$

where ε is compressive strain, f compressive stress, c a constant between 0 and 1, and E_L and F_c are as previously defined. Using the slope of Equation (9–27) in place of E_L in Euler's formula (Eq. (9–25)) leads to Ylinen's buckling equation

$$f_{cr} = \frac{F_c + f_e}{2c} - \sqrt{\left(\frac{F_c + f_e}{2c}\right)^2 - \frac{F_c f_e}{c}} \qquad (9\text{–}28)$$

where F_c is compressive strength and f_e buckling stress given by Euler's formula (Eq. (9–25)). Equation (9–28) can be made to agree closely with Figure 9–7 by choosing $c = 0.97$.

Comparing the fourth-power parabolic function Equation (9–26) to experimental data indicates the function is non-conservative for intermediate L/r range columns. Using Ylinen's buckling equation with $c = 0.8$ results in a better approximation of the solid-sawn and glued-laminated data, whereas $c = 0.9$ for strand lumber seems appropriate.

Built-Up and Spaced Columns

Built-up columns of nearly square cross section with the lumber nailed or bolted together will not support loads as great as if the lumber were glued together. The reason is that shear distortions can occur in the mechanical joints.

If built-up columns are adequately connected and the axial load is near the geometric center of the cross section, Equation (9–28) is reduced with a factor that depends on the type of mechanical connection. The built-up column capacity is

$$f_{cr} = K_f\left[\frac{F_c + f_e}{2c} - \sqrt{\left(\frac{F_c + f_e}{2c}\right)^2 - \frac{F_c f_e}{c}}\right] \qquad (9\text{–}29)$$

where F_c, f_e, and c are as defined for Equation (9–28). K_f is the built-up stability factor, which accounts for the efficiency of the connection; for bolts, $K_f = 0.75$, and for nails, $K_f = 0.6$, provided bolt and nail spacing requirements meet design specification approval.

If the built-up column is of several spaced pieces, the spacer blocks should be placed close enough together, lengthwise in the column, so that the unsupported portion of the spaced member will not buckle at the same or lower stress than that of the complete member. "Spaced columns" are designed with previously presented column equations, considering
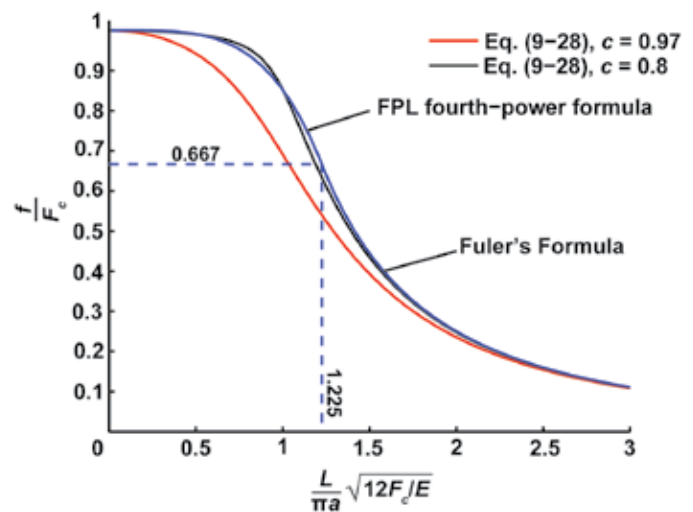

Figure 9–7. Graph for determining critical buckling stress of wood columns.

each compression member as an unsupported simple column; the sum of column loads for all the members is taken as the column load for the spaced column.

Columns with Flanges

Columns with thin, outstanding flanges can fail by elastic instability of the outstanding flange, causing wrinkling of the flange and twisting of the column at stresses less than those for general column instability as given by Equations (9–25) and (9–26). For outstanding flanges of cross sections such as I, H, +, and L, the flange instability stress can be estimated by

$$f_{cr} = 0.044E\frac{t^2}{b^2} \qquad (9\text{–}30)$$

where E is column modulus of elasticity, t thickness of the outstanding flange, and b width of the outstanding flange. If the joints between the column members are glued and reinforced with glued fillets, the instability stress increases to as much as 1.6 times that given by Equation (9–30).

Bending

Beams are subject to two kinds of instability: lateral–torsional buckling and progressive deflection under water ponding, both of which are determined by member stiffness.

Water Ponding

Roof beams that are insufficiently stiff or spaced too far apart for their given stiffness can fail by progressive deflection under the weight of water from steady rain or another continuous source. The critical beam spacing S_{cr} is given by

$$S_{cr} = \frac{m\pi^4 EI}{\rho L^4} \qquad (9\text{–}31)$$

where E is beam modulus of elasticity, I beam moment of inertia, ρ density of water (1,000 kg m^{-3}, 0.0361 lb in^{-3}), L beam length, and $m = 1$ for simple support or $m = 16/3$ for

Table 9–2. Effective length for checking lateral–torsional stability of beams[a]

Support	Load	Effective length L_e
Simple support	Equal end moments	L
	Concentrated force at center	$\dfrac{0.742L}{1-2\,h/L}$
	Uniformly distributed force	$\dfrac{0.887L}{1-2\,h/L}$
Cantilever	Concentrated force at end	$\dfrac{0.783L}{1-2\,h/L}$
	Uniformly distributed force	$\dfrac{0.489L}{1-2\,h/L}$

[a]These values are conservative for beams with a width-to-depth ratio of less than 0.4. The load is assumed to act at the top edge of the beam.

fixed-end condition. To limit the effect of ponding, the beam spacing must be less than S_{cr}.

Lateral–Torsional Buckling

Because beams are compressed on the concave edge when bent under load, they can buckle by a combination of lateral deflection and twist. Because most wood beams are rectangular in cross section, the equations presented here are for rectangular members only. Beams of I, H, or other built-up cross section exhibit a more complex resistance to twisting and are more stable than the following equations would predict.

Long Beams—Long slender beams that are restrained against axial rotation at their points of support but are otherwise free to twist and to deflect laterally will buckle when the maximum bending stress f_b equals or exceeds the following critical value:

$$f_{bcr} = \frac{\pi^2 E_L}{\alpha^2} \tag{9–32}$$

where α is the slenderness factor given by

$$\alpha = \sqrt{2\pi}\sqrt[4]{\frac{EI_y}{GK}}\frac{\sqrt{L_e h}}{b} \tag{9–33}$$

where EI_y is lateral flexural rigidity equal to $E_L\,hb^3/12$, h is beam depth, b beam width, GK torsional rigidity defined in Equation (9–9), and L_e effective length determined by type of loading and support as given in Table 9–2. Equation (9–32) is valid for bending stresses below the proportional limit.

Short Beams—Short beams can buckle at stresses beyond the proportional limit. In view of the similarity of Equation (9–32) to Euler's formula (Eq. (9–25)) for column buckling, it is recommended that short-beam buckling be analyzed by

using the column buckling criterion in Figure 9–7 applied with α in place of L/r on the abscissa and f_{bcr}/F_b in place of f_{cr}/F_c on the ordinate. Here F_b is beam modulus of rupture.

Effect of Deck Support—The most common form of support against lateral deflection is a deck continuously attached to the top edge of the beam. If this deck is rigid against shear in the plane of the deck and is attached to the compression edge of the beam, the beam cannot buckle. In regions where the deck is attached to the tension edge of the beam, as where a beam is continuous over a support, the deck cannot be counted on to prevent buckling and restraint against axial rotation should be provided at the support point.

If the deck is not very rigid against in-plane shear, as for example standard 38-mm (nominal 2-in.) wood decking, Equation (9–32) and Figure 9–7 can still be used to check stability except that now the effective length is modified by dividing by θ, as given in Figure 9–8. The abscissa of this figure is a deck shear stiffness parameter τ given by

$$\tau = \frac{S G_D L^2}{EI_y} \tag{9–34}$$

where EI_y is lateral flexural rigidity as in Equation (9–33), S beam spacing, G_D in-plane shear rigidity of deck (ratio of shear force per unit length of edge to shear strain), and L actual beam length. This figure applies only to simply supported beams. Cantilevers with the deck on top have their tension edge supported and do not derive much support from the deck.

Interaction of Buckling Modes

When two or more loads are acting and each of them has a critical value associated with a mode of buckling, the combination can produce buckling even though each load is less than its own critical value.

The general case of a beam of unbraced length l_e includes a primary (edgewise) moment M_1, a lateral (flatwise) moment M_2, and axial load P. The axial load creates a secondary moment on both edgewise and flatwise moments due to the deflection under combined loading given by Equation (9–7). In addition, the edgewise moment has an effect like the secondary moment effect on the flatwise moment.

The following equation contains two moment modification factors, one on the edgewise bending stress and one on the flatwise bending stress that includes the interaction of biaxial bending. The equation also contains a squared term for axial load to better predict experimental data:

$$\left(\frac{f_c}{F_c}\right)^2 + \frac{f_{b1} + 6(e_1/d_1)f_c(1.234 - 0.234\theta_{c1})}{\theta_{c1}F'_{b1}}$$
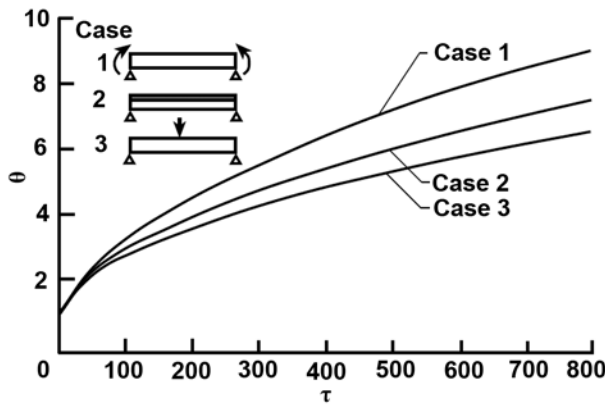$$+ \frac{f_{b2} + 6(e_2/d_2)f_c(1.234 - 0.234\theta_{c2})}{\theta_{c2}F'_{b2}} \le 1.0 \tag{9–35}$$

Figure 9–8. Increase in buckling stress resulting from attached deck; simply supported beams. To apply this graph, divide the effective length by θ.

where f is actual stress in compression, edgewise bending, or flatwise bending (subscripts c, b1, or b2, respectively), F buckling strength in compression or bending (a single prime denotes the strength is reduced for slenderness), e/d ratio of eccentricity of the axial compression to member depth ratio for edgewise or flatwise bending (subscripts 1 or 2, respectively), and θ_c moment magnification factors for edgewise and flatwise bending, given by

$$\theta_{c1} = 1 - \left(\frac{f_c}{F_{c1}''} + \frac{S}{S_{cr}} \right) \quad (9\text{–}36)$$

$$\theta_{c2} = 1 - \left(\frac{f_c}{F_{c2}''} + \frac{f_{b1} + 6(e_1/d_1)f_c}{F_{b1}''} \right) \quad (9\text{–}37)$$

$$F_{c1}'' = \frac{0.822E}{(l_{e1}/d_1)^2} \quad (9\text{–}38)$$

$$F_{c2}'' = \frac{0.822E}{(l_{e2}/d_2)^2} \quad (9\text{–}39)$$

$$F_{b1}'' = \frac{1.44E}{l_e} \frac{d_2}{d_1} \quad (9\text{–}40)$$

where l_e is effective length of member and S and S_{cr} are previously defined ponding beam spacing.

Literature Cited

Maki, A.C.; Kuenzi, E.W. 1965. Deflection and stresses of tapered wood beams. Res. Pap. FPL–RP–34. Madison, WI: U.S. Department of Agriculture, Forest Service, Forest Products Laboratory. 56 p.

Murphy, J.F. 1979. Using fracture mechanics to predict failure of notched wood beams. In: Proceedings of first international conference on wood fracture; 1978 August 14–16; Banff, AB. Vancouver, BC: Forintek Canada Corporation. 159: 161–173.

Newlin, J.A.; Gahagan, J.M. 1930. Tests of large timber columns and presentation of the Forest Products Laboratory column formula. Tech. Bull. 167. Madison, WI: U.S. Department of Agriculture, Forest Service, Forest Products Laboratory. 44 p.

Norris, C.B. 1950. Strength of orthotropic materials subjected to combined stresses. Rep. 1816. Madison, WI: U.S. Department of Agriculture, Forest Service, Forest Products Laboratory. 40 p.

Ylinen, A. 1956. A method of determining the buckling stress and the required cross-sectional area for centrally loaded straight columns in elastic and inelastic range. Zurich, Switzerland: Publication of the IABSA (International Association for Bridge and Structural Engineering). Vol. 16.

Additional References

ASTM. [Current edition]. Standard methods for testing clear specimens of timber. ASTM D 143–94. West Conshohocken, PA: American Society for Testing and Materials.

Bohannan, B. 1966. Effect of size on bending strength of wood members. Res. Pap. FPL–RP–56. Madison, WI: U.S. Department of Agriculture, Forest Service, Forest Products Laboratory. 30 p.

Gerhardt, T.D.; Liu, J.Y. 1983. Orthotropic beams under normal and shear loading. American Society of Civil Engineers (ASCE). Journal of Engineering Mechanics. 109(2): 394–410.

Kuenzi, E.W.; Bohannan, B. 1964. Increases in deflection and stress caused by ponding of water on roofs. Forest Products Journal. 14(9): 421–424.

Liu, J.Y. 1980. Shear strength of wood beams: a Weibull analysis. American Society of Civil Engineers (ASCE). Journal of Structural Division. 106(ST10): 2035–2052.

Liu, J.Y. 1981. Shear strength of tapered wood beams. American Society of Civil Engineers (ASCE). Journal of Structural Division. 107(ST5): 719–731.

Liu, J.Y. 1982. A Weibull analysis of wood member bending strength. Transactions, American Society of Mechanical Engineers. Journal of Mechanical Design. 104: 572–579.

Liu, J.Y. 1984. Evaluation of the tensor polynomial strength theory for wood. Journal of Composite Materials. 18(3): 216–226. (May).

Liu, J.Y.; Cheng, S. 1979. Analysis of orthotropic beams. Res. Pap. FPL–RP–343. Madison, WI: U.S. Department of Agriculture, Forest Service, Forest Products Laboratory. 37 p.

Malhorta, S.K.; Sukumar, A.P. 1989. A simplified procedure for built-up wood compression members. Annual conference. St. John's, Newfoundland: Canadian Society for Civil Engineering: 1–18 (June).

Newlin, J.A.; Trayer, G.W. 1924. Deflection of beams with special reference to shear deformations. Rep. 180.

Washington, DC: U.S. National Advisory Committee on Aeronautics. 18 p.

Rammer, D.R.; Soltis, L.A. 1994. Experimental shear strength of glued-laminated beams. Res. Rep. FPL–RP–527. Madison, WI: U.S. Department of Agriculture, Forest Service, Forest Products Laboratory. 40 p.

Rammer, D.R.; Soltis, L.A.; Lebow, P.K. 1996. Experimental shear strength of unchecked solid sawn Douglas-fir. Res. Pap. FPL–RP–553. Madison, WI: U.S. Department of Agriculture, Forest Service, Forest Products Laboratory. 35 p.

Soltis, L.A.; Rammer, D.R. 1997. Bending to shear ratio approach to beam design. Forest Products Journal. 47(1): 104–108.

Trayer, G.W. 1930. The torsion of members having sections common in aircraft construction. Rep. 334. Washington, DC: U.S. National Advisory Committee on Aeronautics. 49 p.

Trayer, G.W.; March, H.W. 1931. Elastic instability of members having sections common in aircraft construction. Rep. 382. Washington, DC: U.S. National Advisory Committee on Aeronautics. 38 p.

Zahn, J.J. 1973. Lateral stability of wood beam-and-deck systems. American Society of Civil Engineers (ASCE). Journal of Structural Division. 99(ST7): 1391–1408.

Zahn, J.J. 1986. Design of wood members under combined loads. American Society of Civil Engineers (ASCE). Journal of Structural Engineering. 112(ST9): 2109–2126.

Zahn, J.J. 1988. Combined-load stability criterion for wood beam-columns. American Society of Civil Engineers (ASCE). Journal of Structural Engineering. 114(ST11): 2612–2628.